

# Dynamic Analysis of 3 Point Bend Specimens under High Loading Rates

Moon-Sik Han\* and Jae-Ung Cho\*\*

\* Faculty of Automotive Engineering, Keimyung University, Taegu, South Korea

\*\* Department of Automobile, Chonan National Technical College, Chonan, South Korea

## ABSTRACT

Computer simulations of the mechanical behavior of 3 point bend specimens with a quarter notch under impact load are performed. This validity is found to be identified by the experimental proof. The cases with various loading rates applied at the side of the specimen are considered. An elastoplastic von Mises material model is chosen. Gap opening displacement, reaction force, crack tip opening displacement and strain rate are also compared with rate dependent material(visco-plastic material). The stability during various dynamic load can be seen by using the simulation of this study. These differences of the cases with various loading rates are also investigated.

**Keywords :** Dynamic Fracture, gap opening displacement, crack tip opening displacement, strain rate, visco-plastic material

## 1. Introduction

In experiments and analyses of dynamic fracture, three point bend specimens are popularly used as in the finite element analyses by Kalthoff<sup>(1)</sup>, Kanninen<sup>(2)</sup>, Rosakis<sup>(3)</sup>, Van Elst<sup>(4)</sup>, and Ahmad<sup>(5)</sup>.

Most experiments have been performed by using the drop weight which applies a load to the middle point(position) of a specimen(Point A in Fig.2).

However, loading rates are somewhat limited in many published experiments. Therefore, high speed track with high performance<sup>(6)</sup> is used to investigate dynamic fracture behavior of structure under high loading rate. The high speed track used by Wahlborg<sup>(6)</sup> can produce impact speeds in the range of 10m/s to 60m/s.

In this paper, computer simulations are investigate the dynamic behavior of popularly used three-bend specimens under various loading rates. The simulations include plasticity and visco-plasticity

behavior of the specimen material. The stability in dynamic fracture of the material is also considered.

## 2. Finite Element Model

We make numerical simulation by using ABAQUS, commercial FEM code<sup>(7)</sup>. An elastoplastic von Mises model is assumed for mild steel specimens used in this research which have following physical properties:

Young's Modulus(E) = 206 GPa.

Poisson's Ratio( $\nu$ ) = 0.3,

Density( $\rho$ ) = 7800 Kg/m<sup>3</sup>

Yielding stress( $\sigma_Y$ ) = 360 MPa

The brittleness and ductility are clearly shown at the fracture surface of the thick specimen applied to

high loading rate<sup>(8)</sup>. The influence of thickness is rarely shown at the fracture surface of the thin specimen applied to high loading rate. Therefore, the thickness of specimen can be determined as thin as 18 mm. Fig. 2 shows the shape of the specimen which has a crack which size is a quarter of its height.

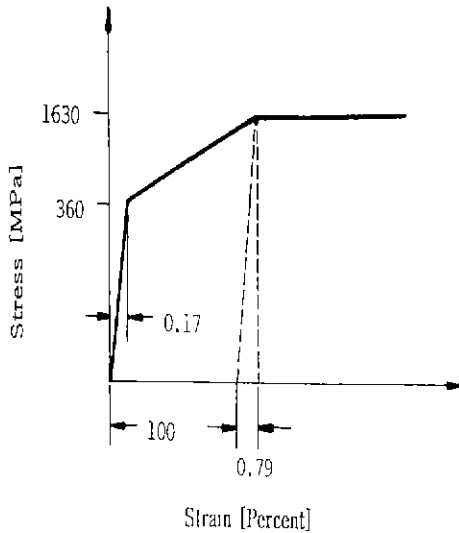


Fig. 1 Static stress-strain curve of the material of a three-point specimen used in our research

(Unit:mm)

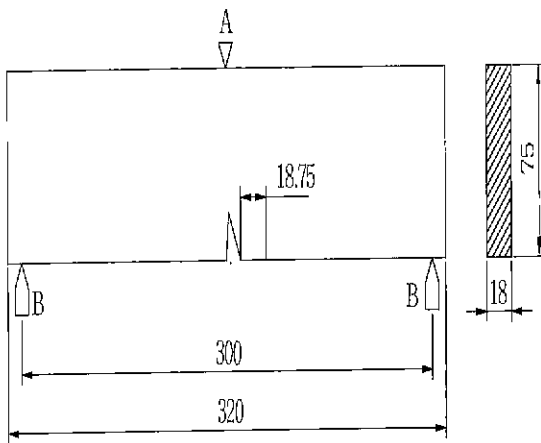


Fig. 2 Three point bend specimen with a quarter notch

Half of the specimen is considered in the

computer simulation because of its geometric symmetry. We choose a two-dimensional finite element model with 92 of 8 node points in our simulation as shown in Fig. 3. Furthermore, one side of eight node point elements near a crack tip concentrates on the crack tip. The impact in dynamic fracture experiment<sup>(9)</sup> causes a specimen to rebound in the air by very small amount. The rebound makes a gap between load and support points which is called gap opening displacement. We compute the gap opening displacement and reaction forces on gap elements and the results are shown in Fig. 3.

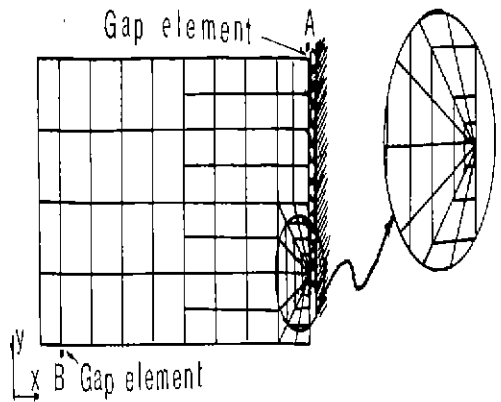


Fig. 3 The finite element model

### 3. Boundary Conditions, Visco-Plasticity and Inspection of Specimen Model

Dynamic load is applied to the imaginary point B on the model as shown in Fig. 3.

The dynamic load is 196kN and the impact-starting time at the impact head is considered to be 'zero'. load rates(V) are taken as 15, 30, 45 and 60m/s. The loading rate is assumed to remain constant after being applied at '0' time.

Simulation is performed for the period from '0' to 600μ s over which crack does not propagate. In this

simulation, we assume the velocity-dependent material characteristic used in Malvern visco-elastic model, one-dimensional from<sup>(10)</sup> of which is

$$\epsilon^{ip} = \beta \left( \frac{\sigma}{\sigma_Y} - 1 \right)^n$$

Here,  $\epsilon^{ip}$  is plastic strain,  $\sigma$  stress, and  $\sigma_Y$  yielding stress.  $\beta$  and  $n$  are visco-plastic coefficients which are chosen to be 4000 and 2, respectively<sup>(11)</sup>.

The experimental display is also shown in Fig.4.

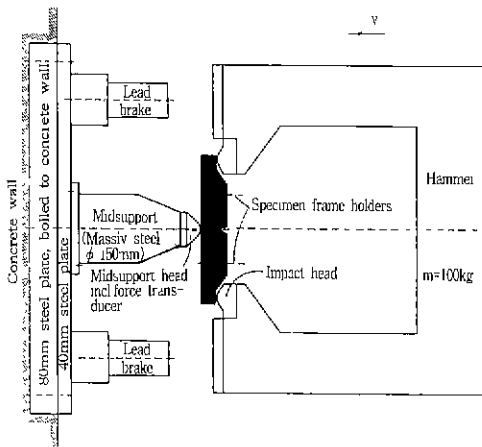


Fig. 4 Cited experimental display

The U-shaped hammer is accelerated to a prescribed velocity and hits the 3PB specimen at its ends. Two hardened and tempered impact heads with cylindrical contact surfaces are attached to the hammer. The experiments of cited paper<sup>(8)</sup> were carried with loading rates of 30 m/s and 45 m/s. The dimensions of designed specimen in this experiment are shown in Fig.5.

The mid-support forces for the simulations together with the experimental result are shown with loading rates of 30 m/sec and 45 m/sec, respectively in Fig. 6 and Fig.7.

The simulation including viscoplastic properties is more close to the experimental result. The simulations

are combinations of with and without rate influence and with and without crack growth.

They are denoted as rate-no rate and crack growth-no crack growth. Good agreement between the experiments and the numerical simulations was obtained for the case of loading rate of 30m/s. The CTODs as function of time are also shown with loading rate of 30 m/sec in Fig. 8.

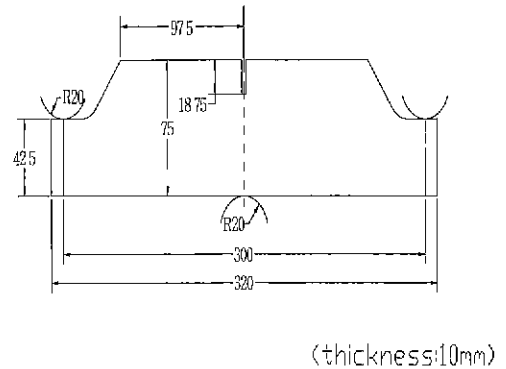


Fig. 5 Dimensions of the new designed 3PB specimens of cited experiment (All dimensions are in mm.)

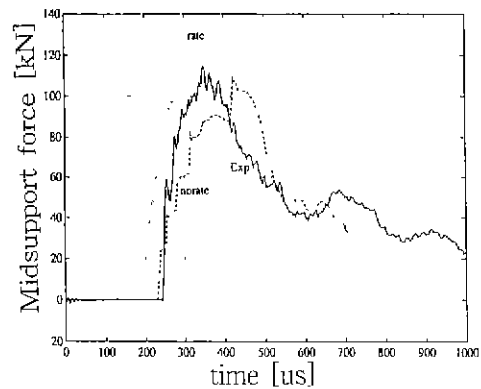


Fig. 6 Mid-support force versus time at 30m/s loading rate for the two different simulations and the experiment (experiment:full line, simulations, no rate: broken line, rate:dotted line)

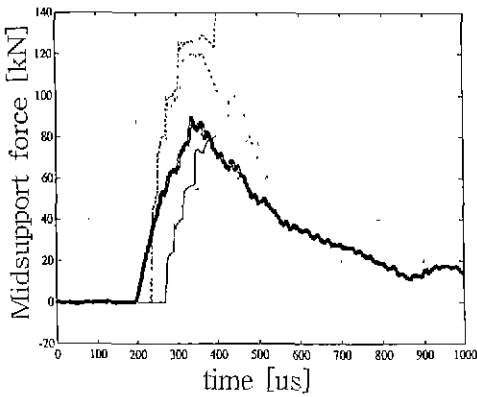


Fig. 7 Mid-support force versus time at 45m/s loading rate for the four different simulations and the experiment (experiment:thick line, simulations, no rate and no crack growth:dotted line, rate and no crack growth:broken line, rate and crack growth:point line)

simulation to the experiment is obtained when viscoplastic and crack propagation properties are included. Therefore, the inspection of this specimen model in this presented paper is sufficient for numerical simulation.

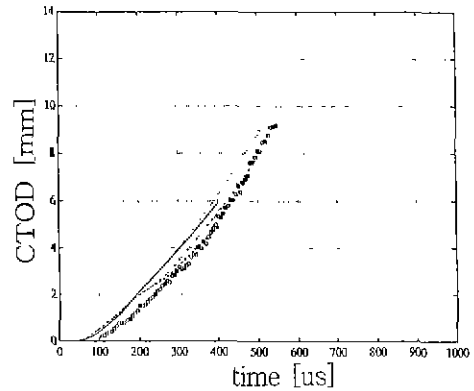


Fig. 9 CTOD at 45m/s loading rate for the four different simulations and the experiment (experiment:circles, simulations, no rate and no crack growth:dotted line, rate and no crack growth:broken line, rate and crack growth:point line)

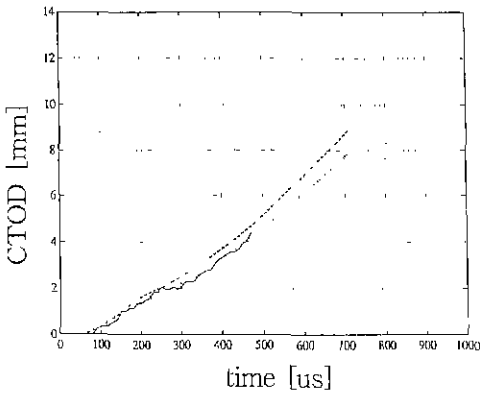


Fig. 8 CTOD at 30m/s loading rate for the two different simulations and the experiment (experiment.full line, simulations, no rate: broken line, rate:dotted line)

As is seen from the figure, the experimental CTOD is close to the simulation including the rate influence. Fig. 9 shows CTOD as a function of time with the loading rate of 45 m/sec. The best fit by the

#### 4. Simulation Results for Dynamic Behavior

Computed gap opening displacements and reaction forces for visco-plastic material are compared with those for non-visco-plastic material. We also investigate the change of crack tip opening displacement (CTOD) and strain rate with time under the various dynamic loadings.

##### 4.1 Reaction Forces and Gap Opening Displacements

Figs. 10~13 show the change of reaction forces at loading point A and supporting point B and Gap Opening Displacement at A for non-visco-plastic specimens with respect to time variation.

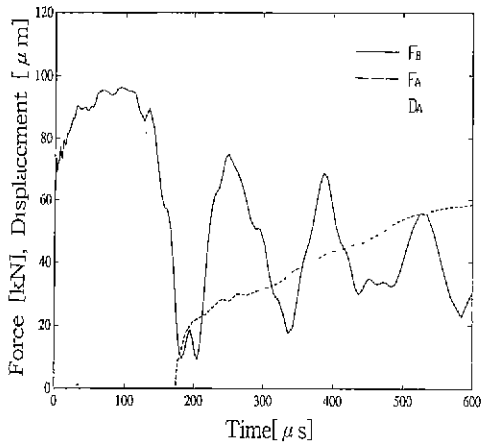


Fig. 10 Dynamic response by impact at the side point B;  $V_B=15\text{m/s}$ (no visco-plasticity)  
 FB=Reaction force at B  
 FA=Reaction force at A  
 DA=Gap opening displacement at A

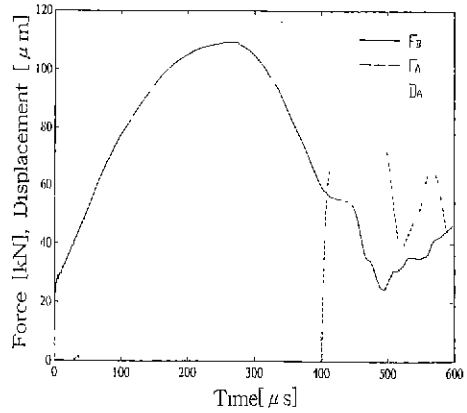


Fig. 12 Dynamic response by impact at the side point B;  $V_B=45\text{m/s}$ (no visco-plasticity)  
 FB=Reaction force at B  
 FA=Reaction force at A  
 DA=Gap opening displacement at A

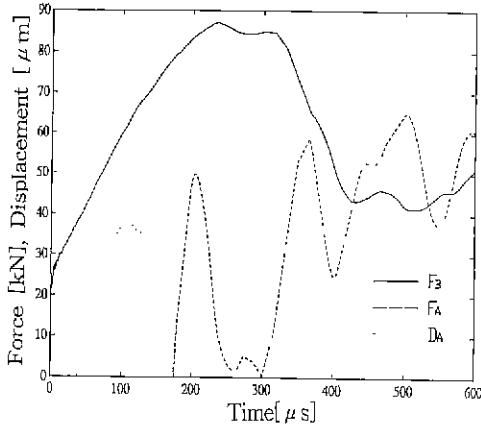


Fig. 11 Dynamic response by impact at the side point B;  $V_B=30\text{m/s}$ (no visco-plasticity)  
 FB=Reaction force at B  
 FA=Reaction force at A  
 DA=Gap opening displacement at A

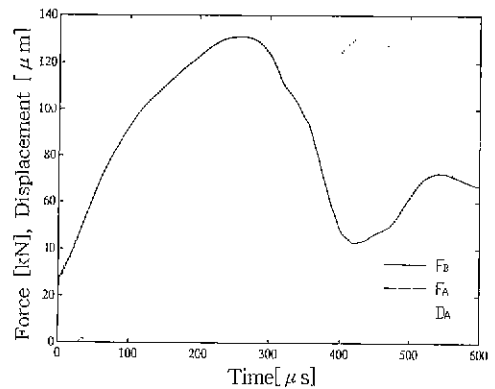


Fig. 13 Dynamic response by impact at the side point B;  $V_B=60\text{m/s}$ (no visco-plasticity)  
 FB=Reaction force at B  
 FA=Reaction force at A  
 DA=Gap opening displacement at A

FB is the reaction force at point B and FA is half the reaction force at point A. Loading rate for

Fig. 10 is 15m/s. FB is suddenly raised to 70kN shortly after impact and increases up to 100kN. Stress wave reaches at the point A 28  $\mu\text{s}$  after impact and induces a small-magnitude reaction force FA at the

point A. The reaction force  $F_A$  holds for about  $10\mu s$  after which the specimen separates from the contact at the point A. Maximum gap opening displacement  $DA$  becomes  $0.094mm$  about  $103\mu s$  later. The gap at point A is closed again  $170\mu s$  after impact.  $F_A$  is rapidly increased to  $20kN$ , and then increases linearly.  $F_B$  vibrates by damping with a period of  $150\mu s$  and the vibrating period decreases slightly with time.

Loading rate in Fig.11 is  $30m/s$ . Maximum reaction force  $F_B$  becomes less than  $90kN$ , and  $F_B$  fluctuates after it becomes about  $50kN$ . Maximum gap opening displacement  $DA$  opens a little wider to become about  $40\mu m$ .

Fig. 12 shows the results for the case of loading rate of  $45m/s$  for which maximum reaction force  $F_B$  becomes larger than  $100kN$  and  $F_A$  drops to less than  $80kN$ . Maximum gap opening displacement  $DA$  widens to  $120\mu m$ .

In Fig. 13 where loading rate is  $60m/s$ ,  $F_B$  rises to about  $130kN$ . Maximum gap opening displacement  $DA$  increases to  $130\mu m$ , and reaction force  $F_A$  does not occur until  $600\mu s$  after impact.

Figs. 14~17 show reaction forces and gap opening displacement with time for visco-plastic specimens.

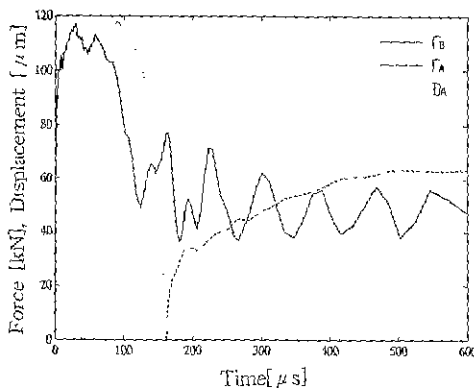


Fig 14 Dynamic response by impact at the side point B;  $VB=15m/s$ (visco-plasticity)  
 $F_B$ =Reaction force at B  
 $F_A$ =Reaction force at A  
 $DA$ =Gap opening displacement at A

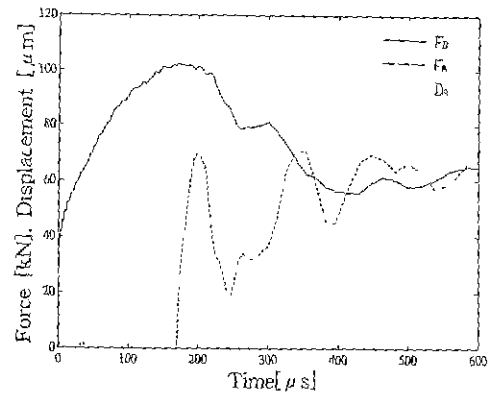


Fig. 15 Dynamic response by impact at the side point B;  $VB=30m/s$ (visco-plasticity)  
 $F_B$ =Reaction force at B  
 $F_A$ =Reaction force at A  
 $DA$ =Gap opening displacement at A

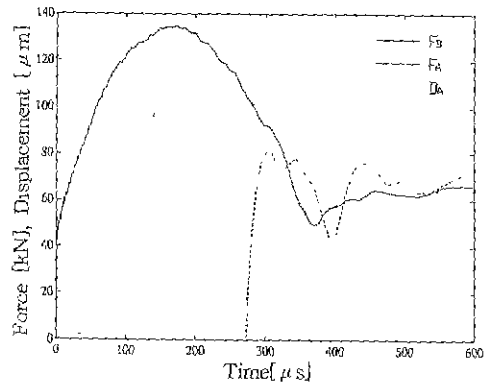


Fig. 16 Dynamic response by impact at the side point B;  $VB=45m/s$ (visco-plasticity)  
 $F_B$ =Reaction force at B  
 $F_A$ =Reaction force at A  
 $DA$ =Gap opening displacement at A

Fig. 14 is the case of loading rate  $15m/s$  for which maximum values of  $F_B$ ,  $DA$ , and  $F_A$  are  $120kN$ ,  $120\mu m$ , and  $60kN$ , respectively. In Fig. 15 with loading rate  $30m/s$ ,  $F_B$  and  $DA$  have maximum values of  $100kN$  and  $60\mu m$ , respectively, and  $F_A$  fluctuates after it reaches the value of  $70kN$ . The loading rate in Fig. 16 is  $45m/s$  for which  $F_B$  and

DA have maximum values of 135kN and 110 $\mu$  m, respectively. Reaction force FA fluctuates after it reaches a value of 80kN. In case of a loading rate of 60m/s as shown in Fig. 17, maximum values of FB, DA, and FA are 150kN, 550 $\mu$ m, and 100kN, respectively.

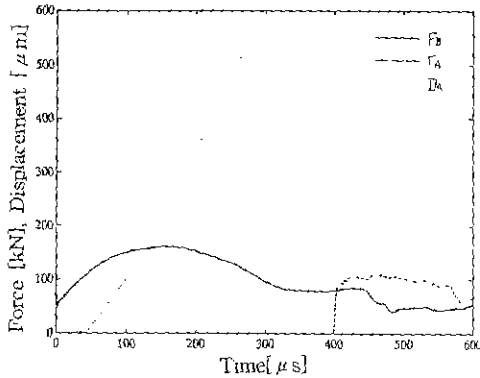


Fig. 17 Dynamic response by impact at the side point B; VB=60m/s(visco-plasticity)  
 FB=Reaction force at B  
 FA=Reaction force at A  
 DA=Gap opening displacement at A

**4.2 Strain rates and CTODs**

Figs. 18~21 show  $\dot{\epsilon}_{xx}$ (strain rate in the x direction) with time of non-visco plastic specimens at positions near the crack tip.

Loading rates for Figs. 18~21 are 15,30,45, and 60m/s, respectively. The positions at the crack tip are denoted by ①, ②, ③, and ④ as in Fig.22.

In Figs. 18~21 and Figs. 23~26 dashed lines(---), solid lines(- -), dotted lines(...), and dot-dashed lines(- · - ·) represent strain rates at the positions ①, ②, ③, and ④, respectively. We can notice that  $\dot{\epsilon}_{xx}$  at the position ① has the largest value and determines the fracture by dynamic crack. The strain rate  $\dot{\epsilon}_{xx}$  is 4300/s at about 150 $\mu$  s with 15m/s in Fig.18, and 1800/s at about 550 $\mu$  s with 30m/s in Fig.19. In Fig. 20 with 45m/s  $\dot{\epsilon}_{xx}$  becomes 25000/s at about 400 $\mu$  s, and in Fig.21 with 60m/s  $\dot{\epsilon}_{xx}$  reaches 35000/s at about 370 $\mu$  s. Figs. 23~26

show  $\dot{\epsilon}_{xx}$  with time of visco-plastic specimens at positions near a crack tip when loading rates are 15m/s, 30m/s, 45m/s, and 60m/s, respectively. The same maximum strain rates( $\dot{\epsilon}_{xx}$ ) of 2800/s occur at 100 $\mu$  s and 250 $\mu$  s in Fig.23 with 15m/s and Fig.24 with 30m/s, respectively. The maximum strain rates in case of 45m/s in Fig.25 and 60m/s in Fig.26 occur at about the same time of 570 $\mu$  s. The maximum  $\dot{\epsilon}_{xx}$  is 3800/s for 45m/s and 5700/s for 60m/s.

Figs. 27 and 28 are crack tip opening displacement(CTOD) curves with time for non-visco plastic specimens and visco-plastic specimens, respectively with loading rates of 15, 30, 45, and 60m/s.

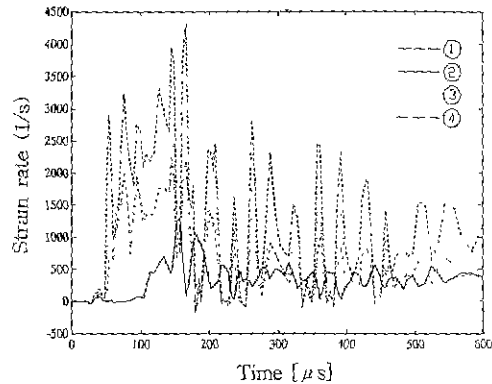


Fig. 18 Strain rate according to time at 1,2,3,4 positions; VB=15m/s(no visco-plasticity)

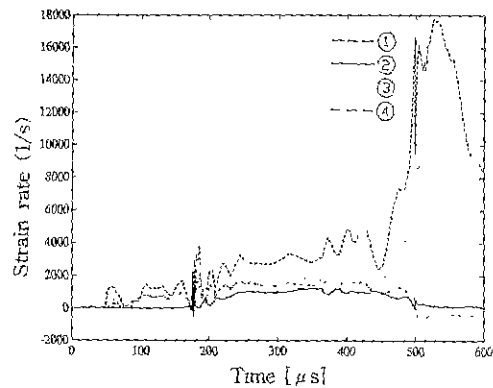


Fig. 19 Strain rate according to time at 1,2,3,4 positions; VB=30m/s(no visco-plasticity)

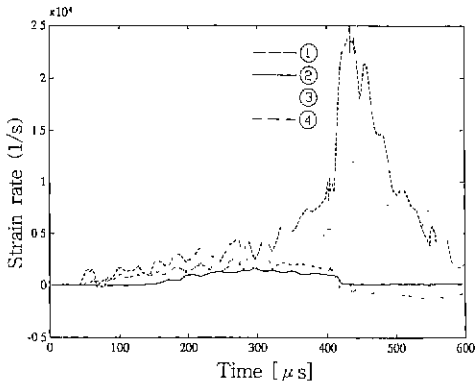


Fig. 20 Strain rate according to time at 1,2,3,4 positions; VB=45m/s(no visco-plasticity)

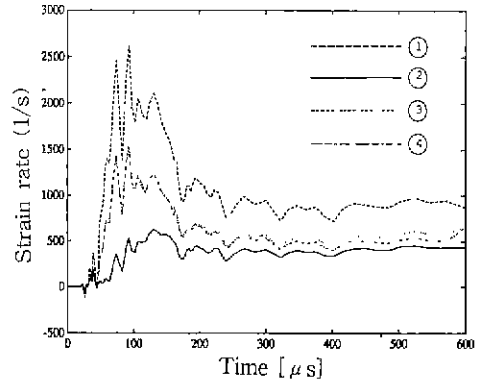


Fig. 23 Strain rate according to time at 1,2,3,4 positions; VB=15m/s(visco-plasticity)

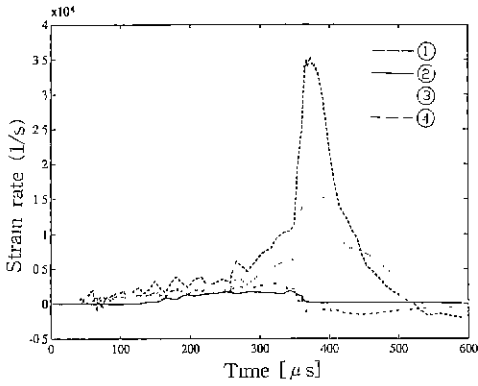


Fig. 21 Strain rate according to time at 1,2,3,4 positions; VB=60m/s(no visco-plasticity)

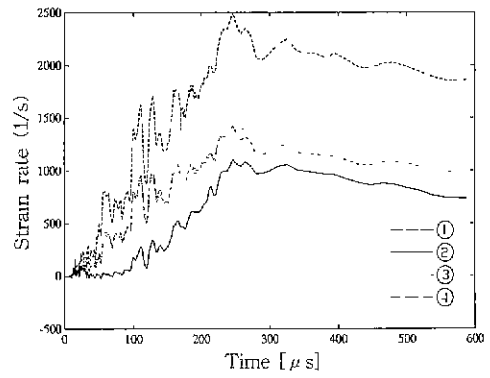


Fig. 24 Strain rate according to time at 1,2,3,4 positions; VB=30m/s(visco-plasticity)

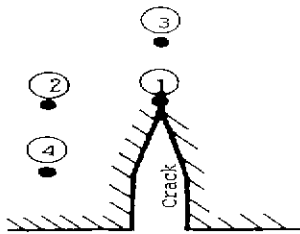


Fig. 22 The positions near crack tip

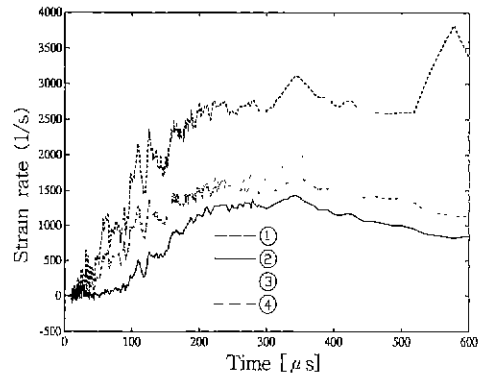


Fig. 25 Strain rate according to time at 1,2,3,4 positions; VB=45m/s(visco-plasticity)



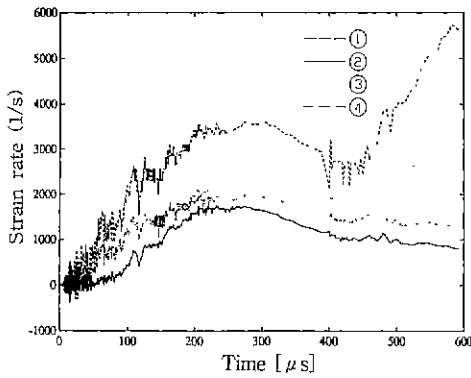


Fig. 26 Strain rate according to time at 1,2,3,4 positions; VB=60m/s(visco-plasticity)

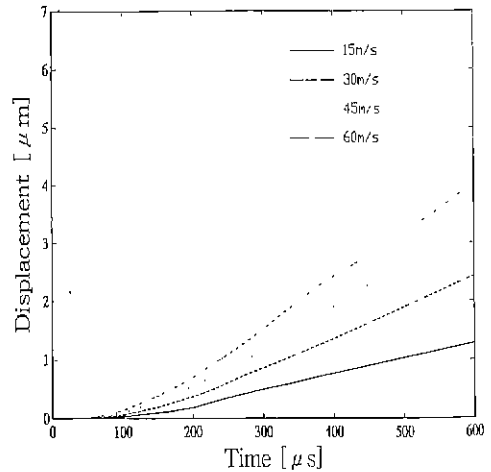


Fig. 28 Crack tip opening displacement according to time at various loading rates; VB=15,30,45,60m/s(visco-plasticity)

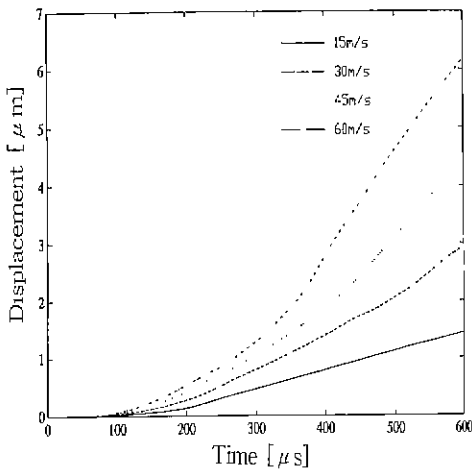


Fig. 27 Crack tip opening displacement according to time at various loading rates; VB=15,30,45,60m/s(no visco-plasticity)

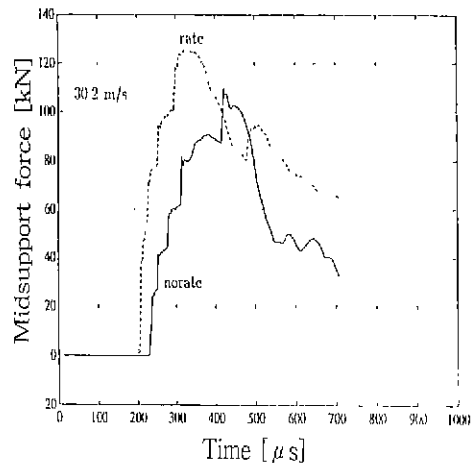


Fig. 29 Influence of the viscoplastic material properties on the midsupport force for 30m/s impact velocity case

Fig. 29 shows the simulation of the midsupport force as a function of time for the The case of loading rate of 30m/s. The notations ( rate and norate) indicate the result from simulations with and without rate depending material properties.

### 5. Considerations

As shown in Figs. 10~17, The reaction forces at impact point B and support point A increase with

dynamic increasing loading rates irrespective of viscoplasticity plasticity of specimens. In particular, reaction forces and gap opening displacements at impacting point B and supporting point A for visco-plastic specimens tend to become higher than those of non-visco plastic specimens

Figs. 18~21 show that maximum strain rates of non-visco plastic specimens increases with increasing

loading rates. The strain rate reaches maximum values in shorter times as loading rates increase.

For visco-plastic specimens as shown in Figs. 23~26, maximum strain rates increase and occur later with loading rates increasing. In general, maximum strain rates for non-visco plastic specimens are much higher than those for visco-plastic specimens. This information on the tendering of strain rates is useful for predicting fracture time by dynamic crack.

From Figs. 27~28, we note that crack tip opening displacement(CTOD) increases with increasing loading rate irrespective of visco-plasticity of material. However, CTOD of a visco-plastic specimen becomes smaller than that of a non-visco plastic specimen. As is seen in Fig. 29, the viscoplasticity reduces the bouncing time of specimen(the time of gap opening displacement;no force growth) and increases the force growth rate when contact is established between the midsupport and the specimen.

## 6. Conclusions

The results of computer simulation analysis for the three point bend specimen of mild steel under various loading rates are summarized as follows:

1) Reaction forces and gap opening displacement at impacting and supporting points of visco-plastic specimens are larger than those of non-visco plastic specimens.

2) The dynamic fracture of material is strongly influenced by the strain rate at the crack tip.

3) As loading rates increase, the maximum strain rates at the crack tips occur earlier for non-visco plastic specimens but occur later for visco-plastic specimens

4) The maximum strain rates and CTOD of visco-plastic specimens are rather smaller than those of non-visco plastic specimens. We can make use of these results in determining stability in dynamic fracture of material.

## References

1. J.F. Kalthoff. "On Some Current Problems in

- Experimental Fracture Dynamics," Workshop on Dynamic Fracture, W.G.Knauss,etc., pp. 11-35, 1983.
2. M.F. Kanninen, et al., "Dynamic Crack Propagation under Impact Loading," Nonlinear and Dynamic Fracture Mechanics, ASME AMD 35, pp. 185-200, 1979.
3. A.J. Rosakis,et al.. "Caustics by Reflection and their Application to ELastic-Plastic and Dynami Fracture Mechanics," SPIE Conference on Photomechanics and Speckle Metrology, San Diego, California, 1988.
4. H.G van Elst, "Assessment of Dynamic Fracture Propagation Resistance at Instrumented High Velocity Gas-gun Impact Tests on SENB-Specimens," ICF 6, Vol. 5, pp. 3089-3097, 1984.
5. J.Ahmad, et al., "Elastic-plastic Finite Element Analysis of Dynamic Fracture," Eng. Frac. Mech., Vol. 17, No. 3 , pp. 235-246. 1983.
6. G.Wihlborg,"Design and Application of a Rig for High Energy Impact Tests," IUTAm Symposium, Tokyo, Japan, 1985.
7. ABAQUS Manual,Version 4.8, Hibbit, Karlsson and Sorensen, Ino. 1989.
8. Ouk S. Lee, et al., "Dynamic Crack Growth in 3PB Ductile Steel Specimen," Proceedings of Asian Pacific Conference for Fracture and Strength'96, pp. 913-916, 1996.
9. A.Bergmark,et al., "Dynamic Crack Propagation in 3PB Ductile Steel Specimens," Technical Report, LUTFD2. TFHF-3045, Lund,Sweden, 1991.
- 10.L.E.MaLvern, "The Propagation of Longitudinal Waves of Plastic Deformation in a Bar of Material Exhibiting a Strain- Rate Effect," J.AppL- Mech. , Vol. 18, pp. 203-208, 1951.
11. B.Brickstad, "A Viscoplastic Analysis of Rapid Crack Propagation Experiments in Steel." J.Mech. Phys. Solids, Vol. 31, No. 4, pp. 307-332.1983.